AIP | Applied Physics Letters

Zincblende-wurtzite phase transformation of ZnSe films by pulsed laser deposition with nitrogen doping

Xiaojun Zhang, Dandan Wang, Matthew Beres, Lei Liu, Zhixun Ma, Peter Y. Yu, and Samuel S. Mao

Citation: Applied Physics Letters **103**, 082111 (2013); doi: 10.1063/1.4819271
View online: http://dx.doi.org/10.1063/1.4819271
View Table of Contents: http://scitation.aip.org/content/aip/journal/apl/103/8?ver=pdfcov
Published by the AIP Publishing

Zincblende-wurtzite phase transformation of ZnSe films by pulsed laser deposition with nitrogen doping

Xiaojun Zhang,[1,2] Dandan Wang,[3,4] Matthew Beres,[1,2] Lei Liu,[3,a)] Zhixun Ma,[1] Peter Y. Yu,[1,5] and Samuel S. Mao[1,2,b)]
[1]*Lawrence Berkeley National Laboratory, Berkeley, California 94720, USA*
[2]*Department of Mechanical Engineering, University of California at Berkeley, Berkeley, California 94720, USA*
[3]*State Key Laboratory of Luminescence and Applications, Changchun Institute of Optics, Fine Mechanics and Physics, Chinese Academy of Sciences, Changchun, 130033, People's Republic of China*
[4]*Graduate School of the Chinese Academy of Sciences, Beijing 100049, People's Republic of China*
[5]*Department of Physics, University of California at Berkeley, Berkeley, California 94720, USA*

(Received 15 July 2013; accepted 12 August 2013; published online 21 August 2013)

Nitrogen-doped ZnSe films have been fabricated by pulsed laser deposition. It is found that the incorporation of nitrogen has resulted in a phase transformation from zincblende to wurtzite. By first-principles total energy calculations, two newly observed Raman peaks at 555 cm^{-1} and 602 cm^{-1} are assigned to vibration modes of N substituting Se in wurtzite and zincblende structures, respectively. This preference of wurtzite phase is consistent with previous prediction of the energy difference ΔE_{WZ-ZB} between wurtzite structure and zincblende structure. This work opens a way to achieve stable ZnSe-based polytypism and may help understand the mechanisms of nitrogen doping in wide-bandgap semiconductors. © *2013 AIP Publishing LLC*.
[http://dx.doi.org/10.1063/1.4819271]

Polytypism is a form of polymorphism in which different structures differ only in stacking sequences of identical, two-dimensional sheets or layers. Zincblende (ZB) and wurtzite (WZ) are the most common polytypes with tetrahedrally bonded covalent structures. Expected to be free of stress and dangling bonds, heterostructures of ZB and WZ polytypes have potential applications in band-structure engineering, spatial localization of electrons and holes, and study of anomalous photovoltaic effect.[1–6] In addition, due to the splitting of valence band maximum in wurtzite structure, the laser threshold of wurtzite ZnSe is usually lower than that of zincblende ZnSe.[7]

While ZB-ZnSe films have been extensively studied, WZ-ZnSe films have been rarely reported due to the difficulty of growing stable WZ-ZnSe films, which caused the difficulty of fabricating ZnSe-based films with polytypism.[8] High-temperature X-ray diffraction (XRD) has shown that the ZB-WZ phase transformation occurred at a high temperature of 1425 °C.[9] There are a few reports of wurtzite ZnSe,[10–12] most of which has been extensively focused on nanostructures. The occurrence of WZ nanostructures can be explained from thermodynamic point of view.[13] The surface energies of {1100} wurtzite planes are lower than {110} and {111} zinc-blende planes.[14] Therefore for nanostructures, in which surface energy plays a more important role, WZ structure becomes more stable than ZB structure. These WZ-ZnSe nanostructures are limited for practical applications where films are needed. It is therefore essential to achieve stable wurtzite ZnSe films. However, there have been no reports on growth of internally stable wurtzite ZnSe films.

The pulsed laser deposition (PLD) system used for this work has been described elsewhere in detail.[15] In order to increase film uniformity, fused quartz and GaAs substrates with stainless steel masks were clamped on a rotatable mounting plate. Before deposition, the chamber was pumped down to a base pressure of 2×10^{-7} Torr and the substrate was heated to 400 °C. The laser fluence on the target and the laser frequency were 2.0 J/cm^2 and 5 Hz, respectively. Nitrogen gas was introduced into deposition chamber by a mass flow controller for nitrogen doping. Crystal structures of the films were analyzed by XRD using Cu Kα radiation. Optical transmission and reflection spectroscopy measurements were performed with a FilmTek 3000PAR SE thin film metrology system, operating in transmission and reflection modes. Film thickness was measured by a Tencor AS500 profilometer. The film thicknesses range from 1.1 μm to 1.4 μm. An ISA Group Horiba microscope Raman system with an internal He-Ne (632 nm) 10 mW laser was used.[16]

Figures 1(b) and 1(c) show XRD patterns of nitrogen-doped ZnSe films grown at 10 mTorr and 40 mTorr, respectively. Compared with other deposition pressures (1 mTorr, 10 mTorr, 500 mTorr), ZnSe films grown at 40 mTorr have better crystallinity, evidenced by a sharpening on the diffraction peaks. The narrow, intense peaks of hexagonal ZnSe (100), (101), (102), and (103) in Figure 1 show that nitrogen doping has turned ZnSe films from cubic to hexagonal phase. Fine XRD scan shows a peak shift of 0.35° to a larger angle, indicating a decrease of lattice constant, which can be explained by the fact that N^{3-} anions are smaller than Se^{2-}. Lattice constants of zincblende- and wurtzite-ZnSe phases are extracted from the diffraction data as follows: $a_{ZB} = 5.65$ Å, $a_{WZ} = b_{WZ} = 4.00$ Å, $c_{WZ} = 6.52$ Å.

Transmittance and reflectance of nitrogen-doped ZnSe films have been measured. Absorption coefficients have been

a)Email: phyliulei@gmail.com.
b)Email: ssmao@berkeley.edu.

calculated using the standard equation $\alpha = -\frac{1}{d}\ln\left(\frac{T}{1-R}\right)$, and plots of $(\alpha dhv)^2$ vs hv are shown in Figure 2. Bandgaps are calculated by linear extrapolation of $(\alpha dhv)^2$ near the band edges. The bandgap decreases by 155 meV from 2.626 eV to 2.471 eV with nitrogen doping, and the absorption edge decreases in sharpness, likely due to nitrogen doping-induced defects.

Figure 3 shows Raman spectra of nitrogen-doped and undoped ZnSe films. 2TA ($\sim$139 cm^{-1}), TO ($\sim$202 cm^{-1}), and LO ($\sim$250 cm^{-1}) peaks of ZnSe films are observed. Two peaks appear at 555 cm^{-1} and 602 cm^{-1} in nitrogen-doped films. It is believed that the peak at 602 cm^{-1} is due to substitution of N on Se sites in ZnSe films. Since nitrogen is much lighter than selenium atom it replaces, its LO phonon frequency of vibration increases by a factor of square root of $\sqrt{\frac{m_{Se}}{m_N}}$ (assuming that the Zn-N spring constant remains the same as Zn-Se) compared to ZnSe. With the Zn-Se LO frequency equal to 250 cm^{-1}, the Zn-N LO frequency is estimated as 594 cm^{-1}, close to 602 cm^{-1} observed in the Raman spectra above.

To better understand the lattice dynamics at the zone center (Γ point) of the Brillouin zone, we carried out first-principles total energy calculations based on Density Functional Theory (DFT) within Perdew-Burke-Ernzerhof (PBE) generalized gradient approximation and the projected augmented wave (PAW) method.[17–20] The dynamical matrix at the Γ point was calculated using the linear response method. Eigenfrequencies and eigenvectors of the lattice vibrations were obtained within the framework of the density functional perturbation theory.[21] A non-analytical correction was used to correct the longitudinal-transverse optical (LO-TO) phonon splitting in the vicinity of the Γ point.[22] The Born effective charges Z*, which are essential for calculating the non-analytical term, were determined.[23] We calculate the zone-center phonon frequencies ω_{LO} and ω_{TO} for ZB-ZnSe as 249 cm^{-1} and 212 cm^{-1}, respectively, which agree very well with the previous experimental and theoretical results.[24,25] To calculate the phonon frequencies of N-doped ZB-ZnSe, a 64-atom supercell was employed. Due to the foreign N-atom, three new phonon modes at 596 cm^{-1}, 392 cm^{-1}, and 391 cm^{-1} emerge for the cubic structure. The

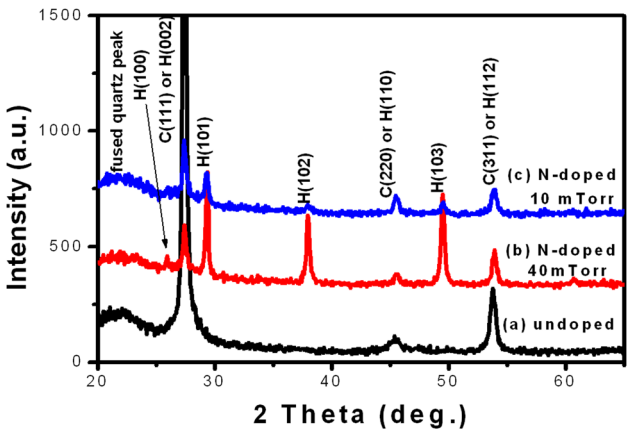

FIG. 1. XRD patterns of (a) an undoped ZnSe film, (b) a nitrogen-doped ZnSe film deposited at an ambient nitrogen pressure of 40 mTorr, and (c) a nitrogen-doped ZnSe film deposited at a pressure of 10 mTorr (C represents cubic phase and H represents hexagonal phase).

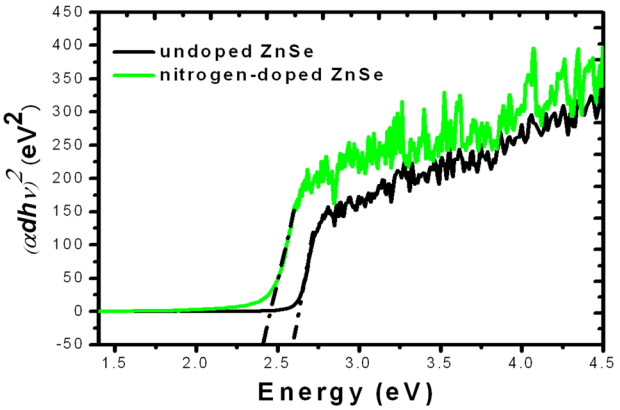

FIG. 2. Plots of $(\alpha dhv)^2$ vs hv for bandgap calculation.

corresponding N vibration modes are represented by the black, green, and red arrows, respectively, in Figure 4(a). The high-frequency stretching vibration at 596 cm^{-1} may characterize the Raman mode observed at 602 cm^{-1} experimentally. Since the nitrogen doping has turned ZnSe films from cubic to hexagonal phase experimentally, we also simulated the N-doped ZnSe in a 72-atom wurtzite-structure supercell. The N vibration modes in the wurtzite supercell are revealed by the phonon frequencies at 537 cm^{-1}, 532 cm^{-1}, and 531 cm^{-1}, which are correspondingly represented by the black, green, and red arrows in Figure 4(b). Apparently, these three N vibrations in wurtzite ZnSe can explain another broad mode around 555 cm^{-1} observed in the Raman spectra. Consequently, based on theoretical results, we can derive that the zincblende and wurtzite phases coexist in the N-doped ZnSe film. It is worth noting that the 10 cm^{-1} difference between the calculated and experimental frequencies of N vibration modes in ZnSe film may originate from the strain effect, as the supercell models do not account for strain.

The occurrence of WZ-ZnSe phase after nitrogen doping is consistent with the previous calculation of Zunger *et al.*[26] The authors have calculated the T = 0 energy difference ΔE_{WZ-ZB} between WZ and ZB structures for binary AB octet compounds using a numerically precise implementation of the first-principles local-density formalism (LDF), including structural relaxations. The phase change of ZnSe films after

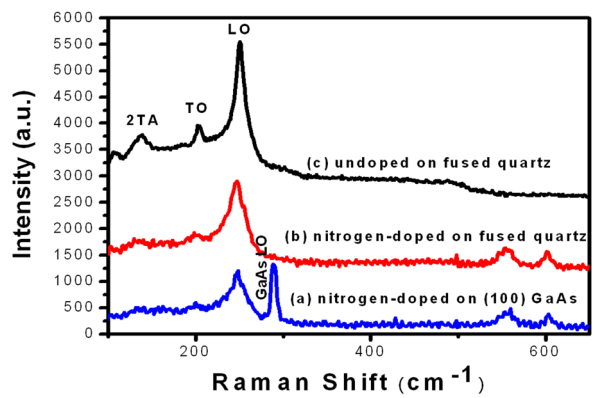

FIG. 3. Raman spectra of (a) a nitrogen-doped ZnSe film on (100) GaAs substrate, (b) a nitrogen-doped ZnSe film on fused quartz substrate, and (c) an undoped ZnSe film on fused quartz substrate.

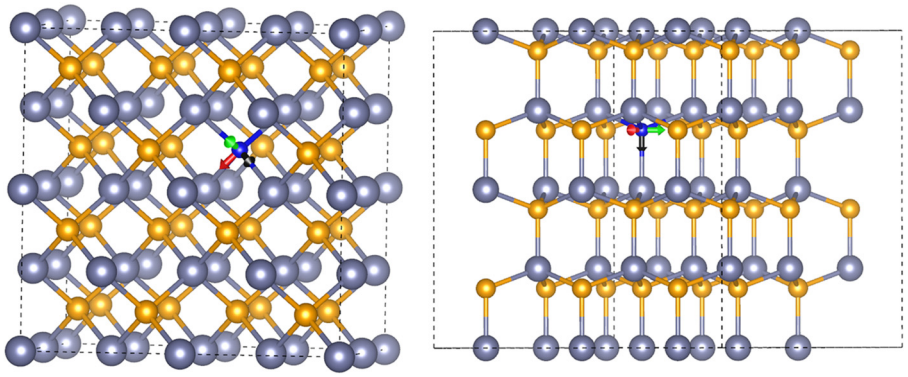

FIG. 4. Structure models of (a) zinc-blende and (b) wurtzite ZnSe:N. The gray spheres represent Zn atoms, the yellow spheres are Se atoms, and the blue spheres stand for N atom. The black, green, and red arrows represent different N vibration modes.

nitrogen doping is consistent with the linear model they proposed to explain the relationship between ΔE_{WZ-ZB} and atomic size difference $|r_A - r_B|$, determined from pseudopotentials. Since Se anions are smaller than N anions, the substitution of Se^{2-} with N^{3-} increases the atomic size difference $|r_A - r_B|$, which based on the linear model will result in a lower energy difference ΔE_{WZ-ZB}, making the wurtzite phase more favorable.

Although the results and analysis above indicate that N has substituted Se on the lattice sites, the nitrogen-doped samples all remain highly resistive. Similar to another II–VI wide-bandgap semiconductor ZnO, this difficulty in p-type doping by nitrogen is believed to be due to compensating defects. These defects may arise from the presence of native defects or other impurities.[27–29] Further, N may introduce local strain when substituting Se, inducing intrinsic defects like vacancies; these defects compensate the N acceptors and make the films non-conductive.

In summary, nitrogen-doped ZnSe films have been obtained by pulsed laser deposition. The incorporation of nitrogen has resulted in a phase transformation from zinc-blende to wurtzite in ZnSe films. XRD results show a decrease in the lattice constant after nitrogen doping. The bandgap decreases by 155 meV from 2.626 eV to 2.471 eV. Two newly observed Raman peaks at 555 cm^{-1} and 602 cm^{-1} are attributed to vibration modes of substituting N in wurtzite and zincblende phases by the first-principles total energy calculations. Although all the results and analysis indicate that N has replaced Se and gone into the lattice sites, the nitrogen-doped ZnSe films are not conductive. This work is of importance to achieve stable WZ ZnSe films for polytypism heterostructures and to understand nitrogen doping difficulties of wide-bandgap semiconductors.

This research has been supported by Office of Nonproliferation and Verification Research and Development, NNSA, of the U.S. Department of Energy, under Contract No. DE-AC02-05CH11231.

[1]Z. Z. Bandicacute and Z. Ikonicacute, Phys. Rev. B **51**, 9806 (1995).
[2]F. Bechstedt and P. Käckell, Phys. Rev. Lett. **75**, 2180 (1995).
[3]O. Brafman, I. T. Steinberger, B. S. Franenke, Z. H. Kalman, and E. Alexander, J. Appl. Phys. **35**, 1855 (1964).
[4]X. H. Lu, P. Y. Yu, L. X. Zheng, S. J. Xu, M. H. Xie, and S. Y. Tong, Appl. Phys. Lett. **82**, 1033 (2003).
[5]G. Shachar and Y. Brada, J. Appl. Phys. **41**, 3127 (1970).
[6]J. Zeman, G. Martinez, P. Y. Yu, and K. Uchida, Phys. Rev. B **55**, R13428 (1997).
[7]A. T. Meney and E. P. O. Reilly, Appl. Phys. Lett. **67**, 3013 (1995).
[8]A. Ohtake, J. Nakamura, M. Terauchi, F. Sato, M. Tanaka, K. Kimura, and T. Yao, Phys. Rev. B **63**, 195325/1 (2001).
[9]I. Kikuma and M. Furukoshi, J. Cryst. Growth **71**, 136 (1985).
[10]Y. Jiang, X. M. Meng, W. C. Yiu, J. Liu, J. X. Ding, C. S. Lee, and S. T. Lee, J. Phys. Chem. B **108**, 2784 (2004).
[11]C. X. Shan, Z. Liu, X. T. Zhang, C. C. Wong, and S. K. Hark, Nanotechnology **17**, 5561 (2006).
[12]Y. C. Zhu and Y. Bando, Chem. Phys. Lett. **377**, 367 (2003).
[13]I. Zardo, S. Conesa-Boj, F. Peiro, J. R. Morante, J. Arbiol, E. Uccelli, G. Abstreiter, and A. F. I. Morral, Phys. Rev. B **80**, 245324 (2009).
[14]F. Glas, J. C. Harmand, and G. Patriarche, Phys. Rev. Lett. **99**, 146101 (2007).
[15]X. Zhang, P. Berdahl, A. Klini, C. Fotakis, and S. S. Mao, Appl. Phys. A **91**, 407 (2008).
[16]J. L. Lei, F. McLarnon, and R. Kostecki, J. Phys. Chem. B **109**, 952 (2005).
[17]G. Kresse and J. Furthmuller, Comput. Mater. Sci. **6**, 15 (1996).
[18]G. Kresse and J. Hafner, Phys. Rev. B **47**, 558 (1993).
[19]G. Kresse and D. Joubert, Phys. Rev. B **59**, 1758 (1999).
[20]J. P. Perdew, K. Burke, and M. Ernzerhof, Phys. Rev. Lett. **77**, 3865 (1996).
[21]X. Gonze and C. Lee, Phys. Rev. B **55**, 10355 (1997).
[22]Y. Wang, J. J. Wang, W. Y. Wang, Z. G. Mei, S. L. Shang, L. Q. Chen, and Z. K. Liu, J. Phys.: Condens. Matter **22**, 202201 (2010).
[23]X. Wu, D. Vanderbilt, and D. R. Hamann, Phys. Rev. B **72**, 035105 (2005).
[24]A. K. Arora, E. K. Suh, U. Debska, and A. K. Ramdas, Phys. Rev. B **37**, 2927 (1988).
[25]A. D. Corso, S. Baroni, R. Resta, and S. de Gironcoli, Phys. Rev. B **47**, 3588 (1993).
[26]C.-Y. Yeh, Z. W. Lu, S. Froyen, and A. Zunger, Phys. Rev. B **46**, 10086 (1992).
[27]B. Theys, V. Sallet, F. Jomard, A. Lusson, J. F. Rommeluere, and Z. Teukam, J. Appl. Phys. **91**, 3922 (2002).
[28]A. Tsukazaki, A. Ohtomo, T. Onuma, M. Ohtani, T. Makino, M. Sumiya, K. Ohtani, S. F. Chichibu, S. Fuke, Y. Segawa, H. Ohno, H. Koinuma, and M. Kawasaki, Nature Mater. **4**, 42 (2005).
[29]C. G. Van de Walle, Phys. Rev. Lett. **85**, 1012 (2000).